

---

# Analytical and variational numerical methods for multiphase flow conservation Instantaneous equation

Zheng He, Xuan Gu, Xiaoyu Sun \*, Jianxin Teng, Binsheng Wang

College of Aerospace and Civil Engineering, Harbin Engineering University, Harbin  
150001 China

\*sunxiaoyu520634@163.com

---

## Abstract

The aim of this paper is to propose a framework to obtain a new formulation for multiphase flow conservation equations without length-scale restrictions, based on the non-local form of the averaged volume conservation equations. The simplification of the local averaging volume of the conservation equations to obtain practical equations is subject to the following length-scale restrictions:  $d \ll \ell \ll L$ , where  $d$  is the characteristic length of the dispersed phases,  $\ell$  is the characteristic length of the averaging volume, and  $L$  is the characteristic length of the physical system. If the foregoing inequality does not hold, or if the scale of the problem of interest is of the order of  $\ell$ , the averaging technique and therefore, the macroscopic theories of multiphase flow should be modified in order to include appropriate considerations and terms in the corresponding equations. In these cases the local form of the averaged volume conservation equations are not appropriate to describe the multiphase system. As an example of the conservation equations without length-scale restrictions, the natural circulation boiling water reactor was consider to study the non-local effects on the thermal-hydraulic core performance during steady-state and transient behaviors, and the results were compared with the classic local averaging volume conservation equations.

---

## 1. Introduction

In a recent paper, Sha and Chao[1] presented a detailed derivation of the porous media formulation for multiphase flow conservation equations. Unfortunately, the derivation is limited to the following length-scale restrictions:  $d \ll \ell \ll L$

where  $d$  is the characteristic length of the dispersed phases,  $\ell$  is the characteristic length of the averaging volume, and  $L$  is the characteristic length of the physical system. According to these authors the length-scale restrictions are inherent in the *local* volume averaging theorem given by Whitaker [2]. In general for a sparsely dispersed flow of a discrete phase, the length-scale restrictions are true.

In earlier studies of the closure problems, Carbonell and Whitaker[3] showed that the average of a spatial deviation.

the position vector relative to the centroid of the averaging volume as illustrated in Fig. 1 (Section 2) under normal circumstances, i.e., in the homogenous regions of the multiphase flow the average deviation is zero.

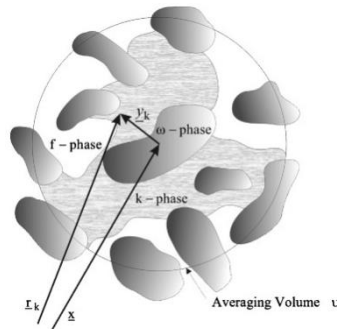


Fig. 1. Position vectors associated with the averaging volume.

In this work we developed applicable averaged transport equations for multiphase flow without length-scale restrictions. This formulation is based on the *non-local* form of the volume-averaged conservation equations.

## 2. Preliminaries

The method of volume averaging is a technique that can be used to rigorously derive continuum equations for multiphase systems. This means that equations which are valid for a particular phase can be spatially smoothed to produce equations that are valid everywhere[4-20], except in the boundaries which contain the multiphase systems.

As mentioned above  $v$  is a constant, which is invariant in both space and time, and its orientation relative to inertial frame of reference fixed, as illustrated in Fig. 1.

The natural circulation model of the NRBWR numerical code was considered in this analysis in order to evaluate the effects of the non-local parameters. Balancing the gravity head available and total loop pressure drop obtained by integration of the momentum balance leads to the model for the natural circulation. The natural circulation model includes the pressure drops and flows from the downcomer, lower and upper plenum (known as chimney), reactor core and steam separators, in order to obtain the following momentum balance. The flow path of the NRL is shown in Fig. C.1.

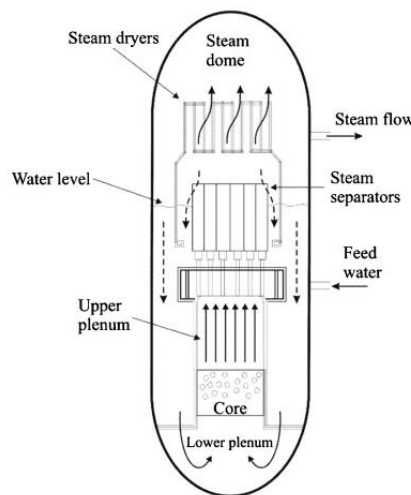


Fig. C.1. NRBWR configuration and flow paths [5]

Fig. C.2 is a schematic diagram of the boiling water reactor where the arrangement of the computational cells of the NRBWR model is shown. The reactor vessel was divided into five zones. Two of these zones, the vessel dome and the downcomer, have a variable volume according to the vessel water level. The three fixed volume zones are the lower plenum, the upper plenum and steam separators, and the reactor core. Due to its importance on the model performance, the latter was subdivided into twelve one-dimensional nodes.

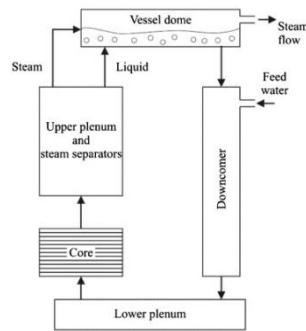


Fig. C.2. Arrangement of the computational nodes in the NRBWR model [5].

### 3. Simulation And Conclusion

Fig. C.3, Fig. C.4, Fig. C.5, Fig. C.6, Fig. C.7 ; Fig. C.8 shows the transient behaviors of the core performance of the SBWR during a reactor Scram for  $\eta'_{za}=0$ ,  $\eta'_{za}=2$  and  $\eta'_{za}=4$ . It is important to note that the classic formulation does not have the term given by Eq.(C.45). The core flow is major for  $\eta'_{za}=4$  (Fig. C.3) due that the global average void fraction in the core is less (Fig. C.4) therefore it presents less hydraulic resistance, with respect to  $\eta'_{za}=0$  and  $\eta'_{za}=2$ .

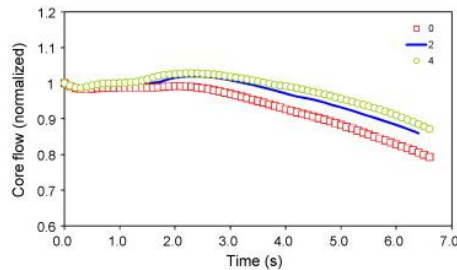


Fig. C.3. Core flow transient behavior for  $\eta'_{za}=0$ ,  $\eta'_{za}=2$  and  $\eta'_{za}=4$ .

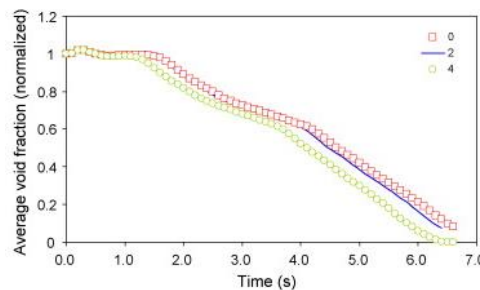


Fig. C.4. Global average void fraction transient behavior for  $\eta'_{za}=0$ ,  $\eta'_{za}=2$  and  $\eta'_{za}=4$ .

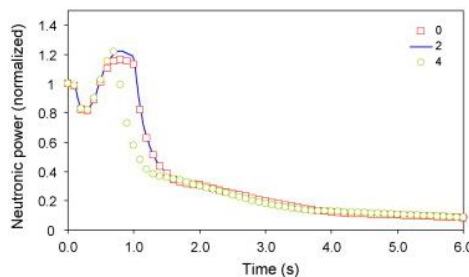


Fig. C.5. Neutronic power transient behavior for  $\eta'_{za}=0$ ,  $\eta'_{za}=2$  and  $\eta'_{za}=4$

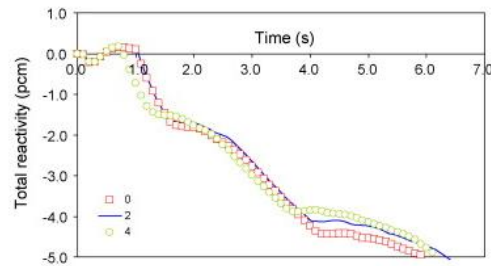


Fig. C.6. Total reactivity during reactor scram for  $\eta'za=0$ ,  $\eta'za=2$  and  $\eta'za=4$ .

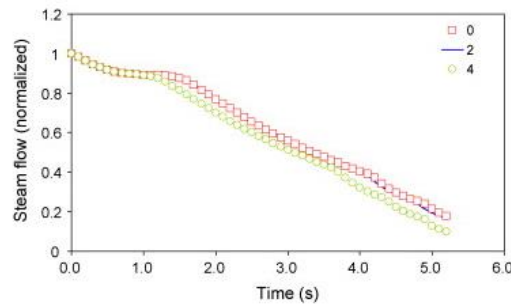


Fig. C.7. Steam flow transient behavior for  $\eta'za=0$ ,  $\eta'za=2$  and  $\eta'za=4$ .

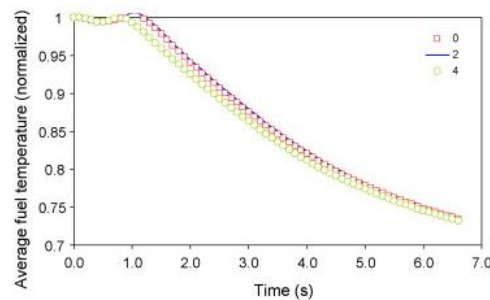


Fig. C.8. Global average fuel temperature transient behavior for  $\eta'za=0$ ,  $\eta'za=2$  and  $\eta'za=4$ .

## Acknowledgements

This work is supported by the National Natural Science Foundation of China(No. 11602066) and the National Science Foundation of Heilongjiang Province of China (QC2015058 and 42400621-1-15047), the Fundamental Research Funds for the Central Universities.

## References

- [1] W.T. Sha, B.T. Chao Novel porous media formulation for mutiphase flow conservation equations Nuclear Eng. Des., 237 (2007), pp. 918–942
- [2] S. Whitaker Advances in theory of fluid motion in porous media Ind. Eng. Chem., 61 (1969), pp. 14–28
- [3] R.G. Carbonell, S. Whitaker Heat and mass transfer in porous media J. Bear, M.Y. Corapcioglu (Eds.), Fundamentals of Transport Phenomena in Porous Media, Martinus Nijhoff, Dordrecht (1984), pp. 123–198
- [4] S. Whitaker The Method of Volume Averaging Kluwer Academic Publishers, The Netherlands (1999)
- [5] G. Espinosa-Paredes, A. Nuñez-Carrera SBWR model for steady state and transient analysis Science and Technology of Nuclear Installations, vol. 2008 (2008) 18 pp. (Article ID 428168)
- [6] S. Sun, M.F. Wheeler Anisotropic and dynamic mesh adaptation for discontinuous Galerkin methods applied to reactive transport Comput. Methods Appl. Mech. Eng., 195 (25–28) (2006), pp. 3382–3405
- [7] S. Sun, M.F. Wheeler Discontinuous Galerkin methods for simulating bioreactive transport of viruses in porous media Adv. Water Resour., 30 (6–7) (2007), pp. 1696–1710

- 
- [8] J. Kou, S. Sun, X. Wang Efficient numerical methods for simulating surface tension of multi-component mixtures with the gradient theory of fluid interfaces *Comput. Methods Appl. Mech. Eng.*, 292 (2015), pp. 92–106
- [9] J. Kou, S. Sun Numerical methods for a multi-component two-phase interface model with geometric mean influence parameters *SIAM J. Sci. Comput.*, 37 (4) (2015), pp. B543–B569
- [10] J. Kou, S. Sun Unconditionally stable methods for simulating multi-component two-phase interface models with Peng–Robinson equation of state and various boundary conditions *J. Comput. Appl. Math.*, 291 (1) (2016), pp. 158–182
- [11] Z. Qiao, S. Sun Two-phase fluid simulation using a diffuse interface model with Peng–Robinson equation of state *SIAM J. Sci. Comput.*, 36 (4) (2014), pp. B708–B728
- [12] C. Du, D. Liang An efficient S-DDM iterative approach for compressible contamination fluid flows in porous media *J. Comput. Phys.*, 229 (2010), pp. 4501–4521
- [13] H. Pan, H. Rui A mixed element method for Darcy–Forchheimer incompressible miscible displacement problem *Comput. Methods Appl. Mech. Eng.*, 264 (2013), pp. 1–11
- [14] H. Wang, D. Liang, R.E. Ewing, S.L. Lyons, G. Qin An approximation to miscible fluid flows in porous media with point sources and sinks by an Eulerian–Lagrangian localized adjoint method and mixed finite element methods *SIAM J. Sci. Comput.*, 22 (2) (2000), pp. 561–581
- [15] Z. Chen, G. Huan, Y. Ma *Computational Methods for Multiphase Flows in Porous Media* SIAM Comput. Sci. Eng. Society for Industrial and Applied Mathematics, Philadelphia (2006)
- [16] H. Hoteit, A. Firoozabadi Numerical modeling of two-phase flow in heterogeneous permeable media with different capillarity pressures *Adv. Water Resour.*, 31 (2008), pp. 56–73
- [17] J. Kou, S. Sun Upwind discontinuous Galerkin methods with mass conservation of both phases for incompressible two-phase flow in porous media *Numer. Methods Partial Differ. Equ.*, 30 (5) (2014), pp. 1674–1699
- [18] H. Hoteit Modeling diffusion and gas–oil mass transfer in fractured reservoirs *J. Pet. Sci. Eng.*, 105 (2013), pp. 1–17
- [19] J. Moortgat, A. Firoozabadi Higher-order compositional modeling of three-phase flow in 3D fractured porous media based on cross-flow equilibrium *J. Comput. Phys.*, 250 (2013), pp. 425–445
- [20] O. Polívka, J. Mikyška Compositional modeling in porous media using constant volume flash and flux computation without the need for phase identification *J. Comput. Phys.*, 272 (2014), pp. 149–169